European Journal of Mechanics A/Solids 28 (2009) 428–432

Contents lists available at ScienceDirect

European Journal of Mechanics A/Solids

www.elsevier.com/locate/ejmsol

Overspeed burst of elastoviscoplastic rotating disks: Part II – Burst of a superalloy turbine disk

M. Mazière [a,*], J. Besson [a], S. Forest [a], B. Tanguy [a], H. Chalons [b], F. Vogel [b]

[a] MINES ParisTech, MAT–Centre des Matériaux, CNRS UMR 7633, BP 87, 91003 Evry Cedex, France
[b] TURBOMECA F-64511 Bordes, France

ARTICLE INFO

Article history:
Received 9 July 2008
Accepted 6 October 2008
Available online 17 October 2008

Keywords:
Stability
Bifurcation
Non-linear behavior
Rotating disks
Spin-softening
Computational mechanics
Nickel based superalloys

ABSTRACT

Burst of a turbo-engine disk in case of overspeed is investigated both from experimental and computational point of view. Two twin disks made of the same nickel based superalloy are tested. For the first one (B-disk), rotation rate in increased till burst. The second one (S-disk) is kept safe by stopping rotation just before burst, and unloading it to measure residual deformations. The material model parameters are deduced either from simple tension tests, or using an inverse method on the S-disk test. Two corresponding finite element simulations of the B-disk are then performed, using either an arc-length control method to overcome the limit point, or dynamic simulations. In both cases, the numerical burst rotation rate, associated with the loss of stability of the structure, is found to be in good agreement with the experimental result.

1. Introduction

During design of turbo-engines, regulation rules require to demonstrate a significant reserve factor between operating rotation rate and burst rotation rate of critical parts such as disks. Experimental tests are performed on disks in order to validate this reserve factor. Predictions of this experimental bursting speed could be useful to analyze tests and reduce development time. Many methods have been developed for that purpose. First, analytical calculations of deformations in rotating disks have been performed for simple geometries and material behavior. A semi-empirical criterion, based on the calculation of the average hoop stress, has been proposed in Robinson (1944). It is still used to estimate burst speed of disks. But because of complex geometries and material models, this criterion is not precise enough, and numerical finite element simulations are nowadays performed to solve this problem. In the companion paper (Maziere et al., 2008), we have investigated the stability of rotating disks. Two main results were presented in this paper: (I) The overspeed burst rotation rate of a rotating disk can be associated with his loss of stability. This limit rotation rate can be estimated from finite element simulation using either an arc-length control method. In case of a viscoplastic material behavior or dynamic simulations, post-processing tools has been used to estimate the loss of stability of disks. (II) The prediction of the overspeed burst rotation rate highly depends on the characterization of the material behavior. The yield surface and hardening law have to be particularly well described in order to obtain an accurate estimate of this rotation rate.

Analytical solutions of disks with simple geometries are available in Love (1927), Timoshenko and Goodier (1934) for elastic material and in Laszlo (1948) for material with permanent deformations. They provide informations on the stress and strain states in rotating disks. An experimental study of burst strength of disks of uniform thickness is performed in Percy and Ball (1974). Experimental results are compared with analytical solutions and with the semi-empirical criterion proposed by Robinson (1944): a disk will burst when the average hoop stress equals the tensile strength of the material. Still on the same geometry, Tvergaard (1978) performed numerical computations of elastoplastic disks. This latter article focuses on the possibility of bifurcation away from the axisymmetric state, in order to determine if this phenomenon may occur before the maximum rotation rate. All these studies have been performed on axisymmetric disks with simple geometries (rectangle or trapezoidal sections). Actual turbo-engines disks shapes are usually less regular and sometimes non-axisymmetric. Experimental disks used to validate numerical predictions of burst rotation rate are of complex shape with holes and notches. It has been shown in Maziere et al. (2008), Maziere (2006) that empirical criteria are inappropriate to predict the limit load of such disks.

Among turbo-engines, one can make a difference between turbofans (aircraft engines) and turboshafts (helicopter engines). The purpose of a turbofan is to produce thrust by accelerating air through the fan and the engine, while the role of a turboshaft is

* Corresponding author. Tel.: +33 1 60 76 30 45.
E-mail address: maziere@mat.ensmp.fr (M. Mazière).

0997-7538/$ – see front matter
doi:10.1016/j.euromechsol.2008.10.002

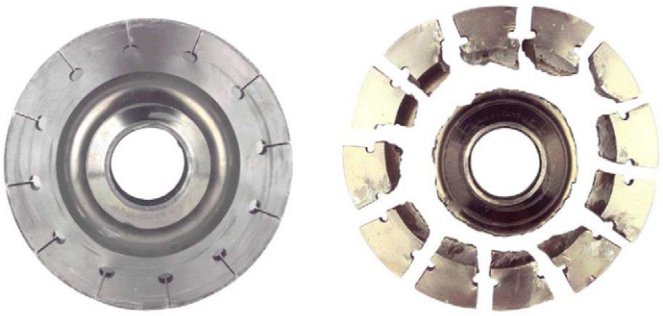

Fig. 1. Photographs of S-disk and B-disk after experiments.

to drive an external rotor. The size and nominal angular velocity of disks also differ. In this paper, an example is given of a test turboshaft disk, which is smaller but rotates faster than turbofan disks. This one is designed in Udimet 720, a nickel based superalloy. Helicopter engines are usually composed of two main turbines. The first one, called "high pressure turbine", is devoted to the production of a flow at a very high speed level from the combustion of high pressure gas. The second one called "power turbine" converts gas flow into rotating power at a very high spin rate.

The aim of this work is to validate the method of prediction based on finite element simulations of the burst rotation rate of elastoplastic experimental disks with complex geometries as proposed in part I (Maziere et al., 2008). For that purpose, two twin experimental disks have been manufactured. The disk denoted B-disk has burst after increasing the rotation rate linearly. The experimental burst rotation rate denoted ω^{EXP} has been measured. The disk denoted S-disk has been stopped at $\omega^{S} = 0.95\omega^{\mathrm{EXP}}$. Inelastic deformations have been measured in order to validate the material behavior. Photographs of the disks after experiments are given in Fig. 1. In this study, finite element simulations are performed on the S-disk in order to validate parameters of the elastoplastic material model. The same model is then used to predict the numerical bursting speed of the B-disk.

Finite element simulations are performed with Zset program (Besson and Foerch, 1997) with a large strain elastoplastic material model presented in Section 2 of part I. Parameters of the model are fitted from simple tensile tests on smooth axisymmetric specimens cut in a third disk. Simple tensile tests on notched axisymmetric specimens (NT) are also performed. Validation of parameters is provided from finite element simulations of notched tensile tests and of the S-disk experiment. Special attention is given to the yield criterion by the introduction of an equivalent stress according to Hosford (1972). Then the numerical burst rotation rate ω^{NUM} of the B-disk is evaluated, using an arc-length control method (Riks, 1979) to overcome the maximal rotation rate. Burst of disk is assumed to coincide with the loss of stability of the structure provided by the global stability condition of (Hill, 1958, 1959; Nguyen, 2000), and then with the maximum of the equilibrium curve. Finally experiments are simulated accounting for inertial terms. Bursts speeds for experiment, static and dynamic simulations are compared for the B-disk.

2. Identification and validation of material parameters

2.1. Identification from smooth tensile specimens

An isotropic elastoplastic model for Udimet 720 at room temperature is proposed in this section. Since deformations of disks are finite, the centrifugal load varies with the rotation rate ω but also with the radius variation of material points. Therefore, finite element simulations have been performed using a finite strain formulation for the material model. Constitutive equations are based on the use of a local objective frame as described in part I (Maziere et al., 2008).

Table 1
Parameters for the nickel based superalloy at 20 °C.

Elasticity		Density		Hardening 1		Hardening 2	
E	200 GPa	ρ	8080 kg m^{-3}	Q_1	2391 MPa	Q_2	−1353 MPa
ν	0.3			b_1	11.1	b_2	17.8
R_0	1211 MPa						

Tensile tests on smooth specimens at different global applied strain rates reveal that yield stress and hardening are: (i) little sensitive to strain rate, (ii) non-linear with two distinct regimes in term of hardening, the stress/strain curve is flat and then hardening. An elastoplastic model is then proposed as follows. The strain rate is split into elastic and plastic contributions. The evolution of the plastic part $\dot{\underset{\sim}{\boldsymbol{e}}}^{p}$ is given by the yield function $f(\underset{\sim}{\boldsymbol{s}}, R)$. The equivalent stress s_{eq} considered is the one proposed in Hosford (1972) and will be discussed further. Finally a non-linear hardening law $R(p)$ is retained with two terms (one for each range of deformation).

$$\dot{\underset{\sim}{\boldsymbol{e}}} = \dot{\underset{\sim}{\boldsymbol{e}}}^{e} + \dot{\underset{\sim}{\boldsymbol{e}}}^{p}, \tag{1}$$

$$f(\underset{\sim}{\boldsymbol{s}}, R) = s_{\mathrm{eq}} - R(p), \tag{2}$$

$$s_{\mathrm{eq}} = \left[\frac{(\sigma_1-\sigma_2)^n + (\sigma_2-\sigma_3)^n + (\sigma_1-\sigma_3)^n}{2}\right]^{1/n} \tag{3}$$

where $\sigma_1 \geqslant \sigma_2 \geqslant \sigma_3$ are the principal stresses and $1 \leqslant n \leqslant \infty$,

$$R(p) = R_0 + Q_1\left(1 - \mathrm{e}^{-b_1 p}\right) + Q_2\left(1 - \mathrm{e}^{-b_2 p}\right), \tag{4}$$

$$\dot{\underset{\sim}{\boldsymbol{e}}}^{p} = \dot{p}\frac{\partial f}{\partial \underset{\sim}{\boldsymbol{s}}}, \quad \dot{p} \geqslant 0, \tag{5}$$

$$\underset{\sim}{\boldsymbol{s}} = 2\mu\underset{\sim}{\boldsymbol{e}}^{e} + \lambda\,\mathrm{tr}(\underset{\sim}{\boldsymbol{e}}^{e})\underset{\sim}{\mathbf{1}}. \tag{6}$$

The Poisson ratio ν and the density of Udimet 720 have been obtained from literature. Other parameters of the model have been identified from a tensile test on a smooth specimen for a global applied strain rate equal to 10^{-3} s^{-1}. Since there is no softening on the conventional stress/strain curve and no necking on tensile specimens (deformations remain homogeneous), the true tensile curve can be plotted easily up to specimen fracture. The Young's modulus E and the yield stress R_0 are identified from the elastic part of the curve, while the hardening law is provided by the plastic range of the curve. The convexity change of curves is made from a combination between an hardening and a softening term in function $R(p)$. Softening parameters, with subscript 2, affect mostly the beginning of the plastic range (up to 5%). Hardening parameters, with subscript 1, affect the whole plastic range. Finally, only the parameter n in the equivalent stress s_{eq} is left undetermined and will be identified below. All other parameters are given in Table 1.

2.2. Identification from notched tensile specimens

Simulations of experiments on smooth and notched tensile specimens have first been performed using the von Mises equivalent stress in the yield criterion. For smooth specimens, the global experimental strain stress curves are obviously accurately reproduced. Indeed, parameters have been calibrated from these curves. However, simulations of notched tensile specimens then overestimate the global stress level (see Fig. 2). Same simulations have then performed with Tresca equivalent stress. Results were found in better agreement with experimental curves even if they lightly underestimate the global stress level. Hosford equivalent stress